High pressure study and bonding analysis of $Mg_2Co_3Sn_{10+x}$

G. Krauss *, Q.F. Gu

Laboratory of Crystallography, ETH Zurich, Wolfgang-Pauli-Strasse 10, 8093 Zurich, Switzerland

ARTICLE INFO

ABSTRACT

Intermetallic materials with large unit cells are scientifically interesting and challenging due to their structural and chemical complexity. The investigated hexagonal $Mg_2Co_3Sn_{10+x}$ crystallizes with 120 atoms per unit cell and a unit cell volume of 2655 Å^3. An in-house single-crystal high pressure study was done using a recently developed low background diamond-anvil cell. The investigated compound is structurally stable up to the highest reached pressure of 9.69 GPa. Compressibility measurements revealed the $\vec{c}$-axis to be slightly less compressible than the $\vec{a}$-axis. A chemical bonding analysis based on the analysis of the topology of the electron localization function identified $Mg_2Co_3Sn_{10+x}$ as a compound combining localized and delocalized chemical bonding in its structure. The macroscopic properties of the compound are dominated by the metallic 3D framework, which is also responsible for the anisotropic compressibility.

1. Introduction

Intermetallic compounds, especially those with large unit cells recently gained more and more interest due to their potentially interesting physical properties caused by the presence of different length scales in their structures. These compounds are often built of clusters, i.e. small structural units with length scales typically much smaller than the size of the unit cell. An interesting open question faces the formation and stability of these compounds. Their structural behaviour at non-ambient conditions may give hints for the further understanding of these mechanisms. Studies of complex materials at non-ambient conditions often induces experimental difficulties, as required critical experimental parameters like, e.g. resolution of the experiment or measuring time are at the border of making the study unfeasible. To study materials at high pressures (hp), diamond-anvil cells (DACs) are widely used. Complex intermetallic compounds often show a certain amount of structural disorder, observable by a structured diffuse scattering in the diffraction patterns. In a feasibility study it was shown that it is possible to obtain diffraction images with a comparable amount of information with and without DAC [1]. The change of the design of the DAC, in this case the replacement of polycrystalline Be by single-crystalline diamond further improved the obtainable quality of the data [2,3]. $Mg_2Co_3Sn_{10+x}$ [4] was

chosen for the present single-crystal hp study and bonding analysis, because of the following reasons:

(i) Only a few hp studies on inorganic materials with large unit cells >2000 Å^3 are known to the literature. To the best of our knowledge, no complex intermetallic compounds having these large unit cell sizes were studied so far at hps using single crystals. The title compound crystallizes with 120 atoms per unit cell and a volume of ca. 2600 Å^3. These compounds are still challenging for structural determinations at non-ambient conditions as well as the understanding of the chemical bonding.

(ii) One Sn-site of the structure is statistically underoccupied. It is interesting to see if there will be a structural ordering taking place as a function of pressure. Could this underoccupancy be explained based on the chemical bonding?

(iii) The structure can be seen as a metallic framework with the presence of homoatomic tin bonding, as observed in other tin-rich cobalt stannides. Is there localized and delocalized bonding present in the structure between atoms of the same type and is such a structure stable at elevated pressure?

2. Experimental details

2.1. Sample preparation

Single crystals of $Mg_2Co_3Sn_{10+x}$ were grown as described in [4] from a tin solution using a mixture of Mg, Co and Sn in molar ratio

---

* Corresponding author. Fax: +41 44 632 11 33.
 E-mail address: guenter.krauss@mat.ethz.ch (G. Krauss).

2:3:29. The mixture was filled in an alumina crucible and heated up in 0.5 bar argon atmosphere from ambient temperature to 1123 K within 4 h, kept at 1123 K for 1 h and cooled down to ambient temperature at a rate of 50 K/h. The excess tin was dissolved in half-concentrated (ca. 20%) hydrochloric acid. Black hexagonal platelets of $Mg_2Co_3Sn_{10+x}$ with a typical diameter of about 130 μm and a thickness of about 50 μm were obtained besides CoSn, which formed as a by-product.

2.2. X-ray diffraction

Single-crystal diffraction measurements were done on an Oxford-Diffraction Xcalibur XP diffractometer equipped with an Onyx CCD-detector and Mo-$K\alpha$ radiation (Oxford enhance). A single crystal was selected and first measured without DAC, then mounted into a modified ETH DAC [5] using a Re gasket (thickness 125 μm, hole diameter 250 μm). A ruby sphere was added as pressure sensor and a mixture of methanol and ethanol in volume ratio 4:1 served as pressure transmitting medium. Datasets were collected at several pressures using the following strategy to acquire high-angle data with sufficient redundancy at short data collection times: two ω-scans ($-45° \leqslant \omega \leqslant 0°$) at $\kappa = 0°$, detector at $-25°$, $\phi = 0°$ and $180°$, respectively; two ω-scans ($0° \leqslant \omega \leqslant 45°$) at $\kappa = 0°$, detector at $25°$, $\phi = 0°$ and $180°$, respectively; two ω-scans ($-56.9° \leqslant \omega \leqslant -12°$) at $\kappa = 134.4°$, detector at $0°$, $\phi = -56.9°$ and $123°$, respectively. The step width was $1°$ at exposure times of 40–60 s, resulting in total data collection times of 8–12 h per dataset and pressure. The collected data was corrected for crystal and DAC absorption using the CrysAlis [6] and Absorb6.1 [7] programs, respectively. Outliers caused by the DAC were rejected using Average2.2 [8] and the equations of state calculated using the program Eosfit5.2 [9].

2.3. Calculation procedures

Quantum chemical calculations were performed by the use of the Vienna ab initio simulation package (VASP) [10,11] based on the projected-augmented wave (PAW) function method [12]. The structures were geometry optimized in VASP, which employs ultrasoft pseudo-potentials [13] and the local density approximation (LDA) to model the contribution of the exchange correlation to the total energy and the valence electron density distribution. The kinetic energy cutoff for the runs was chosen to be sufficient to ensure convergence of the energy and the generation of a minimum energy structure using a $3 \times 3 \times 3\Gamma$-centred k-point mesh. Optimization of the structural parameters is performed until the forces on the atoms are less than 0.01 eV/Å, and all stress components are less than 0.002 eV/Å^3. The electron localization function (ELF, η) was evaluated according to [14] with an ELF module already implemented within the VASP. Bader's analysis has been done on a charge density grid calculated with VASP by Bader program [15]. Visualization was performed using the program VESTA [16].

3. Results and discussion

The investigated crystal was first characterized at ambient pressure without DAC. The site occupation of Sn9 was refined to 78%, yielding the composition $Mg_2Co_3Sn_{10.17}$. This site occupation was held fixed for all further refinements at hps. The composition is slightly more Sn-rich compared to the reported values in [4] as could be expected when grown from Sn-flux. The details of the refinement are shown in Table 1, atomic parameters are given in Table 2.

Table 1
Crystallographic and experimental data for the structure refinement of $Mg_2Co_3Sn_{10.17}$ at ambient conditions

|	
Data collection	Oxford-Diffraction Xcalibur XP
Wavelength	0.71073 Å
Crystal system	Hexagonal
Space group	$P6_3/mmc$ (No. 194)
Unit cell	$a = 9.5348(4)$ A
	$c = 33.727(1)$ A
	$V = 2655.4(2)$ A^3
	$Z = 8$
Density, calc.	7.065 g/cm^3
Absorption coefficient	22.13 cm^{-1}
Absorption correction	Empirical
Crystal shape and size	Hexagonal platelet
	$120 \times 120 \times 60$ μm^3
Crystal colour	Black
Index and theta range	$-12 \leqslant h \leqslant 14, -14 \leqslant k \leqslant 13, -51 \leqslant l \leqslant 51$
	$3.45° \leqslant \theta \leqslant 33.14°$
Measured reflections	28,459
Unique reflections	1974
Unique reflections $I > 2\sigma(I)$	1585
Refinement method	Full matrix least squares on F^2
Parameters	69
Goodness of fit	1.173
Final R-indices	$R_i = 0.0613$
	$R_1 = 0.0548, wR_2 = 0.0977 (I > 2\sigma(I))$
	$R_1 = 0.0548, wR_2 = 0.1010$ (all)
Largest diff. peak and hole	3.67 e/Å^3, -3.23 e/Å^3

Table 2
Atomic parameters for $Mg_2Co_3Sn_{10.17}$ at ambient conditions

Atom	site	sof	x	y	z
Sn1	2c	1.000	$\frac{1}{3}$	$\frac{2}{3}$	$\frac{1}{4}$
Sn2	4e	1.000	0	0	0.07563(3)
Sn3	4e	1.000	0	0	0.16115(3)
Sn4	4e	1.000	$\frac{2}{3}$	$\frac{1}{3}$	0.04905(4)
Sn5	4f	1.000	$\frac{1}{3}$	$\frac{2}{3}$	0.15390(4)
Sn6	6h	1.000	0.89075(5)	0.10925(5)	$\frac{1}{4}$
Sn7	12k	1.000	0.55319(4)	0.10637(8)	0.20685(2)
Sn8	12k	1.000	0.10991(8)	0.55496(4)	0.03580(2)
Sn9	12k	0.779(4)	0.85117(6)	0.70235(13)	0.02614(3)
Sn10	24l	1.000	0.00825(6)	0.34631(6)	0.11728(1)
Co1	12k	1.000	0.15837(7)	0.84163(7)	0.05535(3)
Co2	12k	1.000	0.83458(7)	0.16542(7)	0.17646(3)
Mg1	4f	1.000	$\frac{2}{3}$	$\frac{1}{3}$	0.1362(2)
Mg2	12k	1.000	0.6550(4)	0.8275(2)	0.19936(9)

A detailed description of the structure is given in [4]. For a better understanding of the following, the main structural features are reviewed briefly. With respect to binary stannides, the structure is described based on a packing of Co–Sn polyhedra. As shown in Fig. 1 two different Co–Sn polyhedra can be found in the structure. Eight tin atoms (Sn2, Sn8, Sn9, and Sn10) coordinate Co1 as slightly distorted tetragonal antiprism (blue). Eight of these antiprisms are connected via common vertices in a way that their base planes form a slightly distorted cube (Sn9 and Sn2 atoms). Two exo-bonded Sn3 atoms and another tin atom (Sn4) with a radial bond (Sn4–Sn9) vector complete the Co_6Sn_{34}-cluster. Each of these clusters is connected via common vertices to six neighbouring clusters in the (001) plane. The Sn4 atoms bridge three Co_6Sn_{34}-clusters. The second crystallographic independent cobalt atom (Co2) is slightly distorted trigonal prismatically coordinated by six tin atoms. Three prisms share one common vertex, and two of these units are connected by pairwise sharing of adjacent vertices along the $\bar{c}$-direction. Each of the resulting Co_6Sn_{31}-clusters shares common vertices with six neighbours in
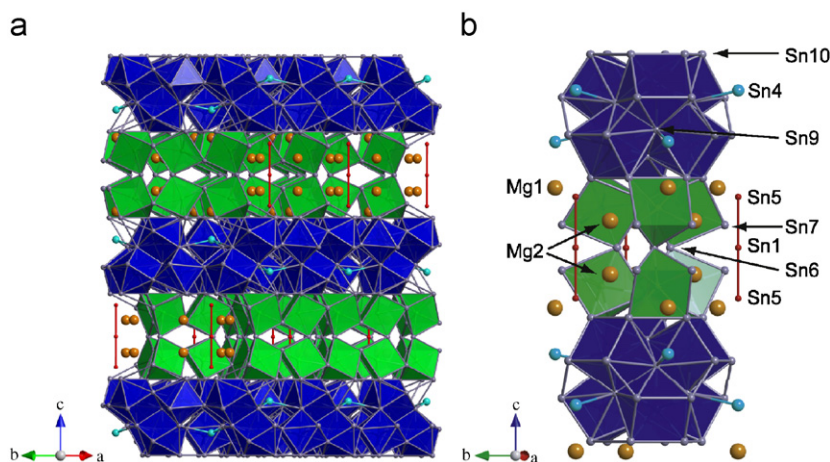
Fig. 1. (Colour online) The crystal structure of $Mg_2Co_3Sn_{10+x}$. (a) The structure can be described as packings of two different types of CoSn polyhedra (blue and green). The underoccupied Sn9 site is located in the blue layer, whereas all Mg atoms are found in the green layer. (b) Packing scheme of the different Co–Sn polyhedra and the linear Sn_3-chain.

the (001) plane. The whole crystal structure can be described as a stacking of these two kinds of layers formed by the Co_6Sn_{34}-cluster and the Co_6Sn_{31}-clusters, respectively. An underoccupied tin site (Sn9) is only found in the layer formed by Co_6Sn_{34}-clusters, whereas magnesium atoms are only present in the other layer. Mg1 completes the coordination sphere of the pseudo-tetrahedrally bonded Sn4 atom. Six Mg2 atoms form a trigonal prism around a linear Sn_3-unit (Sn5–Sn1–Sn5), which is located in a cavity of the packing of Co_6Sn_{31}-clusters (Fig. 1b).

3.1. High pressure study

For the single crystal hp studies a modified ETH DAC was used. This low-background cell uses backing plates made of conically shaped single-crystalline diamonds instead of the commonly used polycrystalline beryllium backing plates. The design is described in detail in [5]. Single-crystal measurements were done up to a pressure of 9.69 GPa. Structure refinements were done at each pressure step. Due to the decrease in data quality at higher pressures the atoms were refined using isotropic ADPs.

The structure is stable up to the highest applied pressures. The lattice parameters are listed in Table 3, structural data for three different pressures is given in Table 4. For further details of the structure refinements at intermediate pressures please refer to the corresponding cif-files. Fig. 2 shows the volume and lattice parameters as a function of pressure with a fitted second-order Birch–Murnaghan equation of state. The bulk modulus at zero pressure was calculated as $K_0 = 75.3(5)$ GPa.[1] At 9.69 GPa the decrease of the unit-cell volume is 10%.

The value of the compressibility is in between the values of the large void compound CoSn ($K_0 = 127(8)$ GPa [17]) and pure Sn ($K_0 = 58.2$ GPa [18]) as could be expected. A comparison to other Co–Sn is due to the lack of data not possible (to the best of our knowledge). The $\vec{c}$-axis is slightly less compressible than the

Table 3
Experimental unit-cell parameters of $Mg_2Co_3Sn_{10.17}$ as a function of pressure

P (GPa)	a (Å)	c (Å)	V (Å^3)
10^{-4}	9.5348(4)	33.727(1)	2655.4(2)
1.429(2)	9.4310(4)	33.460(14)	2577.3(3)
2.837(3)	9.3802(4)	33.302(14)	2537.3(3)
4.150(10)	9.3243(4)	33.186(13)	2498.7(3)
5.287(1)	9.2909(4)	33.015(16)	2468.1(4)
5.862(8)	9.2605(4)	33.028(14)	2452.9(3)
6.940(20)	9.2321(4)	32.860(12)	2425.5(3)
7.800(7)	9.2071(4)	32.798(14)	2407.8(3)
8.601(5)	9.1824(4)	32.732(14)	2390.1(3)
9.688(5)	9.1502(4)	32.622(14)	2365.4(3)

$\vec{a}$-axis, for which values of the compressibilities[2] of $\beta_{0,c} = -3.9(1) \times 10^{-3}$ GPa^{-1} and $\beta_{0,a} = -4.8(1) \times 10^{-3}$ GPa^{-1} are obtained. Accordingly, at the highest applied pressure c is shortened by 3.8% and a by 4.6%, respectively. To understand this small but significant difference, the change of interatomic distances as a function of pressure was analysed in detail. All distances decrease monotonically with increasing pressure. In Table 5 and Fig. 3 the ratio of the interatomic distances at ambient pressure and 9.69 GPa are given.

The dashed lines represent the $\pm 3\sigma$-interval around the average of all observed changes in bond lengths within this interval (marked as a solid line). Obviously four Sn–Sn distances, namely Sn2–Sn3, Sn1–Sn5, Sn7–Sn7, and Sn4–Sn8, and two Mg–Sn distances, Mg1–Sn4 and Mg2–Sn6 change significantly less compared to the average of all the interatomic distances as well as the lattice parameters. Except Sn7–Sn7 and Mg2–Sn6 the other four interatomic vectors have their largest components parallel to the $\vec{c}$-direction (Fig. 4). Therefore it is reasonable that this direction is less compressible than the $\vec{a}$-directions. To understand the structure from a chemical point of view, the chemical bonding was analysed by means of a topological analysis of the ELF.

---

[1] Please note, that the obtained value of the bulk modulus is slightly different compared to the value reported in [5], although both calculations are based on the same measurements. The reason for the difference is that in this study the lattice parameters obtained by the integration of the reflections from the 2D diffraction images were used, which are slightly different compared to those obtained by *peak hunting* [6]. Please note also that the composition given in [5] was not based on a single-crystal refinement, but on the Sn-rich border given in [4], i.e. $Mg_2Co_3Sn_{10.15}$ instead of $Mg_2Co_3Sn_{10.17}$.

[2] The compressibilities of the axes at zero pressure, β_0, were obtained by fitting a second-order Birch–Murnaghan equation of state to the cubes of the lattice parameter values as a function of pressure. The obtained values of 'K_0' were related to β_0 by $\beta_0 = -(3K_0)^{-1} = a_0^{-1}(\partial a/\partial P)_{P=0}$

Table 4
Atomic parameters for $Mg_2Co_3Sn_{10.17}$ as a function of pressure, exemplarily shown for three different pressures. Data for intermediate pressures are given in the corresponding cif files

Atom	$P = 1.429(2)$ GPa			$P = 5.287(1)$ GPa			$P = 9.688(5)$ GPa		
	x	y	z	x	y	z	x	y	z
Sn1	$\frac{1}{3}$	$\frac{2}{3}$	$\frac{1}{4}$	$\frac{1}{3}$	$\frac{2}{3}$	$\frac{1}{4}$	$\frac{1}{3}$	$\frac{2}{3}$	$\frac{1}{4}$
Sn2	0	0	0.0755(3)	0	0	0.0759(3)	0	0	0.0759(4)
Sn3	0	0	0.1615(4)	0	0	0.1619(4)	0	0	0.1619(4)
Sn4	$\frac{2}{3}$	$\frac{1}{3}$	0.0496(4)	$\frac{2}{3}$	$\frac{1}{3}$	0.0502(4)	$\frac{2}{3}$	$\frac{1}{3}$	0.0508(5)
Sn5	$\frac{1}{3}$	$\frac{2}{3}$	0.1531(4)	$\frac{1}{3}$	$\frac{2}{3}$	0.1526(3)	$\frac{1}{3}$	$\frac{2}{3}$	0.1520(4)
Sn6	0.89054(14)	0.10946(14)	$\frac{1}{4}$	0.89050(14)	0.10950(14)	$\frac{1}{4}$	0.89034(18)	0.10966(18)	$\frac{1}{4}$
Sn7	0.55275(11)	0.1055(2)	0.20695(18)	0.55160(11)	0.1032(2)	0.20707(17)	0.55046(13)	0.1009(3)	0.2069(2)
Sn8	0.1097(2)	0.55483(10)	0.03598(18)	0.1088(2)	0.55439(10)	0.03587(17)	0.1083(3)	0.55416(13)	0.0358(2)
Sn9	0.85106(17)	0.7021(3)	0.0262(3)	0.85075(17)	0.7015(3)	0.0261(2)	0.8506(2)	0.7013(4)	0.0261(3)
Sn10	0.00785(15)	0.34612(14)	0.11719(11)	0.00713(14)	0.34589(14)	0.11708(11)	0.00677(18)	0.34577(18)	0.11688(14)
Co1	0.1582(2)	0.8418(2)	0.0554(3)	0.1581(2)	0.8419(2)	0.0555(3)	0.1579(2)	0.8421(2)	0.0557(4)
Co2	0.83469(19)	0.16531(19)	0.1768(3)	0.8349(2)	0.1651(2)	0.1765(3)	0.8347(3)	0.1653(3)	0.1766(4)
Mg1	$\frac{2}{3}$	$\frac{1}{3}$	0.1359(17)	$\frac{2}{3}$	$\frac{1}{3}$	0.1365(14)	$\frac{2}{3}$	$\frac{1}{3}$	0.1391(19)
Mg2	0.6549(10)	0.8274(5)	0.1983(9)	0.6528(9)	0.8264(5)	0.1992(9)	0.6516(12)	0.8258(6)	0.1978(12)
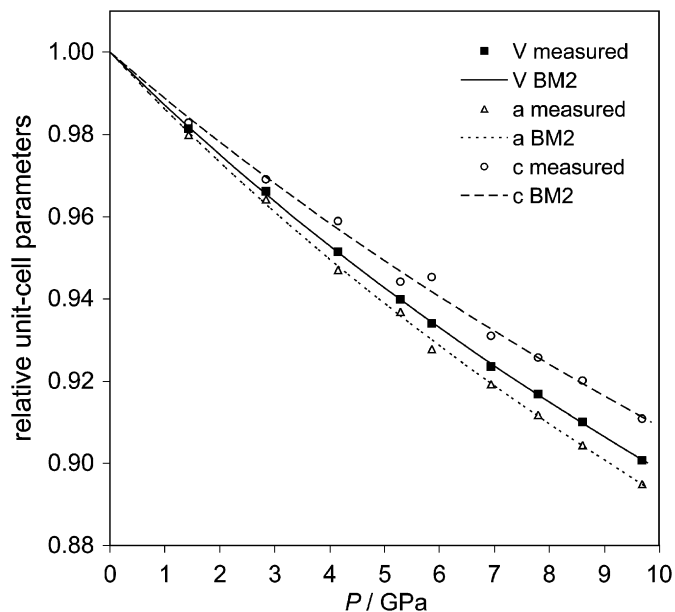
Fig. 2. The normalized unit cell volume and lattice parameters of $Mg_2Co_3Sn_{10.17}$ as a function of pressure. For comparison, the lattice parameters are given as $(a/a_0)^3$ and $(c/c_0)^3$, respectively. The lines represent the best fits of second-order Birch–Murnaghan equations of state. The errors are in the size of the symbols.

3.2. Bonding analysis

The structure of $Mg_2Co_3Sn_{10.17}$ contains one site being partially occupied by tin (Sn9). As partial occupations cannot be handled in the calculations, an idealized model was used. Instead of the rhombohedra formed by Sn2 atoms along the threefold axis and Sn9 forming the six additional corners, an idealized cyclohexyl-type ordered substructure was used. The Sn9 position is occupied by 78% tin for the most tin-rich composition of the compound. The lower limit of the Sn9 occupancy was found to be 67% [4]. This occupation was used for the idealized model, leaving two of the six corners unoccupied. For the model used in the calculations, the idealized cyclohexyl-type substructures at $z \approx 0$ and 0.5 were tilted by an angle of 90°, respectively. Total and partial density of state (DOS) plots are shown in Fig. 5. The total DOS shows a local

Table 5
Selected interatomic distances (<3.75 Å, given in Å) of $Mg_2Co_3Sn_{10.17}$ at ambient pressure and 9.69 GPa.

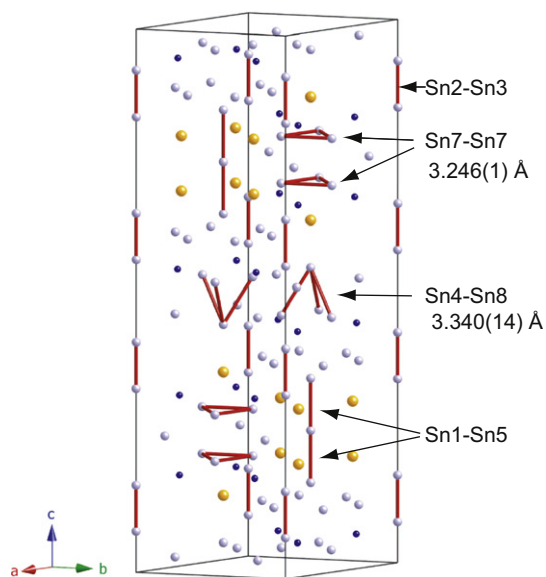| Atoms	Interatomic distances			Atoms	Interatomic distances		
	10^{-4} GPa	9.69 GPa	Ratio		10^{-4} GPa	9.69 GPa	Ratio
Co1–Sn2	2.704(1)	2.587(6)	0.956(3)	Sn7–Sn7	2.911(1)	2.809(14)	0.965(5)
Co1–Sn8	2.618(1)	2.525(5)	0.964(2)	Sn7–Sn7	3.246(1)	3.190(4)	0.983(1)
Co1–Sn9	2.725(1)	2.622(7)	0.962(3)	Sn7–Sn10	3.505(1)	3.382(8)	0.965(2)
Co1–Sn10	2.626(1)	2.521(11)	0.960(5)	Sn8–Sn8	3.021(11)	2.897(11)	0.959(4)
Co2–Sn3	2.780(1)	2.664(5)	0.958(2)	Sn8–Sn8	3.195(1)	3.089(4)	0.967(1)
Co2–Sn6	2.648(1)	2.553(12)	0.964(5)	Sn8–Sn9	3.381(1)	3.248(8)	0.961(3)
Co2–Sn7	2.656(1)	2.561(6)	0.964(3)	Sn8–Sn9	3.411(1)	3.263(2)	0.957(1)
Co2–Sn10	2.616(1)	2.529(10)	0.967(4)	Sn8–Sn10	3.244(1)	3.119(8)	0.961(3)
Sn1–Sn5	3.241(1)	3.197(13)	0.986(4)	Sn9–Sn9	3.025(2)	2.914(12)	0.963(5)
Sn2–Sn3	2.884(2)	2.807(17)	0.949(7)	Sn9–Sn10	3.524(1)	3.389(10)	0.962(3)
Sn2–Sn9	2.971(1)	2.871(9)	0.966(3)	Sn10–Sn10	3.010(1)	2.884(3)	0.958(1)
Sn2–Sn10	3.553(1)	3.407(5)	0.959(2)	Sn10–Sn10	3.145(1)	3.040(3)	0.967(1)
Sn3–Sn6	3.498(1)	3.358(11)	0.960(3)	Sn10–Sn10	3.381(1)	3.226(3)	0.954(1)
Sn3–Sn10	3.583(1)	3.461(6)	0.966(2)	Mg1–Sn4	2.940(7)	2.880(64)	0.978(24)
Sn4–Sn8	3.405(1)	3.340(14)	0.981(4)	Mg1–Sn7	3.031(5)	2.879(48)	0.950(17)
Sn4–Sn8	3.687(1)	3.534(3)	0.959(1)	Mg2–Sn1	3.158(3)	3.043(23)	0.964(8)
Sn4–Sn9	3.144(1)	3.025(6)	0.962(2)	Mg2–Sn3	3.126(3)	2.999(18)	0.959(6)
Sn5–Sn10	3.316(1)	3.176(5)	0.958(2)	Mg2–Sn5	3.067(3)	2.931(23)	0.956(8)
Sn6–Sn6	3.125(2)	3.010(5)	0.963(2)	Mg2–Sn6	3.024(3)	2.957(23)	0.978(9)
Sn6–Sn7	3.520(1)	3.377(4)	0.959(1)	Mg2–Sn7	3.265(2)	3.100(5)	0.950(2)

maximum close to the Fermi level. In the valence region between ca. -3 eV and the Fermi level, the DOS has significant Co d-character. The projected DOS shows a mixing with Sn-p states. The states below -5 eV originate mainly from Sn-s states. These features are comparable to those observed in other ternary stannides, like for example $SrNiSn_2$ [19]. The local maximum at the Fermi level explains the observed Pauli paramagnetism of $Mg_2Co_3Sn_{10+x}$ [4].

Although the crystal structure of $Mg_2Co_3Sn_{10+x}$ is very complex, the ELF shows mainly two interesting features, which are positioned around the two crystallographically independent Mg atoms. As could be expected, these are the most interesting areas with respect to chemical bonding of the structure of $Mg_2Co_3Sn_{10+x}$.

- *Vicinity of Mg1*: Sn4 is coordinated pseudo-tetrahedrally by three Sn9 and one Mg1 atom. In the idealized structure the Sn9
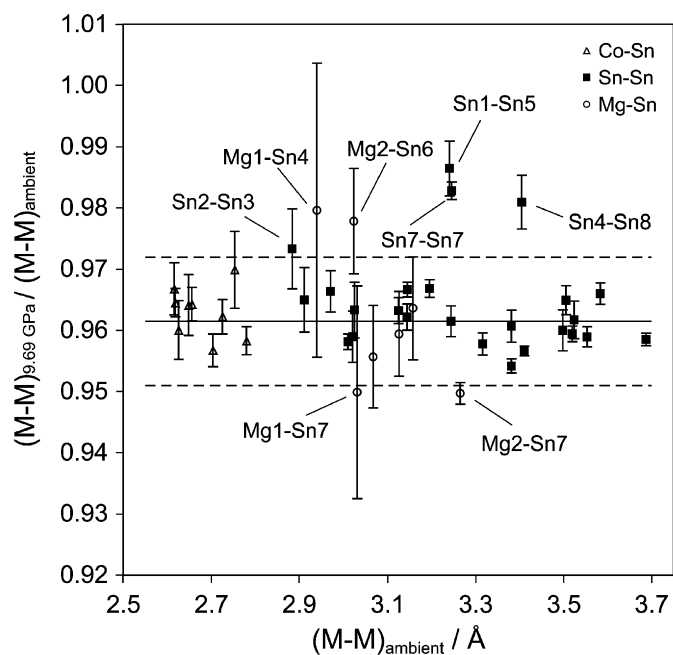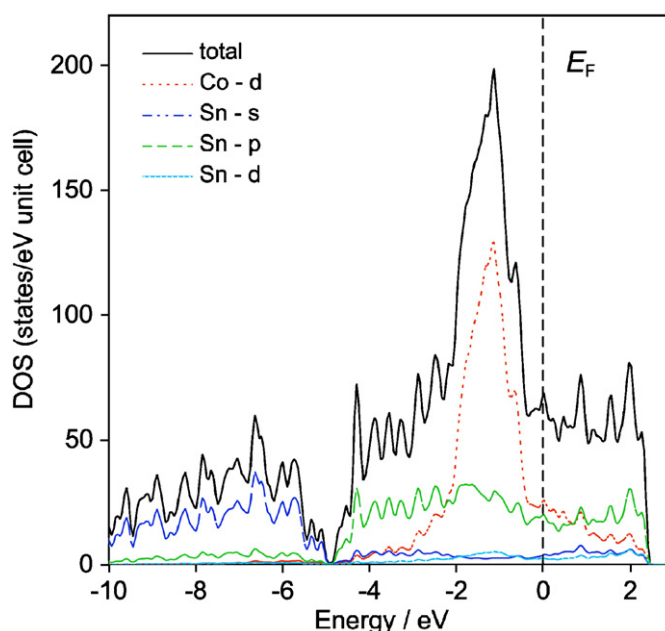
Fig. 3. Relative change of interatomic distances of $Mg_2Co_3Sn_{10.17}$ between ambient pressure and 9.69 GPa. The dashed lines represent the $\pm 3\sigma$-interval around the average value (solid line). Errors in distance are in the size of the symbols.

Fig. 5. (Colour online) Total and projected electronic density of states for $Mg_2Co_3Sn_{10+x}$.

Fig. 4. (Colour online) Interatomic vectors with the smallest changes in length as a function of pressure. The largest components can be observed parallel to the $\vec{c}$-direction, yielding to a lower compressibility along $\vec{c}$ than along $\vec{a}$.

site is occupied only by $\frac{2}{3}$, i.e. one of the three Sn9 sites is empty on average. This structural feature was accommodated for by the used model as described in the previous paragraph. The ELF shows a maximum close to the Sn4 atom, which can be interpreted as a lone pair. It also reveals weak attractors along the Sn4–Sn9 bonds, indicating a small amount of covalent bonding (Fig. 6a,d). The nicely doughnut-shaped bond attractors between the Sn10–Sn10, Sn2–Sn3, and Sn8–Sn8 atoms indicate covalent bonds between these atoms. The valence shell for Mg1 is nearly spherical, suggesting a close-shell

configuration and therefore distinct ionic character. This is represented by the significant positive charge in the order of 1.5 obtained from the Bader analysis (Table 6). Sn4 shows a negative charge of ca. −0.4. The lone pair and formation of two bonds with covalent character between Sn4 and Sn9 could be the reason for the underoccupation of the Sn9 site and the observed phase width of $Mg_2Co_3Sn_{10+x}$ [4]. The phase width of $Mg_2Co_3Sn_{10+x}$ is characterized by an occupation of Sn9 in the range of 0.67 for $x = 0$ to 0.78 for $x = 0.17$, respectively. It can be assumed, that the electrons transferred from Mg1 to Sn4 and the framework enables the formation of a Sn^{1-}-like Sn4 atom in about one out of 10 unit cells for $Mg_2Co_3Sn_{10+x}$ with $x = 0.17$ and none for $x = 0$, respectively. This assumption has to be regarded critically, as the idealized model was chosen for the calculation and the distances of the second-nearest Sn neighbours of Sn4, namely Sn8 are still in a distance, where significant interaction has to be expected (Sn4–Sn9: 3.144(1) Å, Sn4–Sn8: 3.405(1) Å, Table 5).

- *Vicinity of Mg2*: The Mg2 atoms coordinate Sn1 trigonal prismatically. The ELF shows three distinct maxima around the Sn1 atom, which is the central atom of the linear chain Sn5–Sn1–Sn5 (Fig. 6b). These maxima indicate lone pairs directed towards the centres of the edges of the trigonal prism formed by the six Mg2 atoms. No bond attractors are observed between the Sn1 and Sn5 atoms, indicating no covalent single bond. Three small ELF maxima are present around the Sn5 atoms directed towards the Mg atoms. At lower ELF values, the maxima tend to spread out and partly overlap, as can be seen in the cross section through the linear chain (Fig. 6d). Additional maxima can be found in the vicinity of Sn6, located towards the edges of the trigonal Mg2-prism. The maxima in the vicinity of Sn1 and Sn6 as well as the centres of the edges of the trigonal Mg2-prisms lie on a virtual line connecting Sn1 and Sn6. Like observed for Mg1, the valence shell of Mg2 is nearly spherical, emphasizing its ionic character (charge 1.5). Sn1 has a distinct negative charge of ca. −1.22 and also Sn5 and Sn6 show negative charges of −0.66 and −0.43, respectively (Table 6).
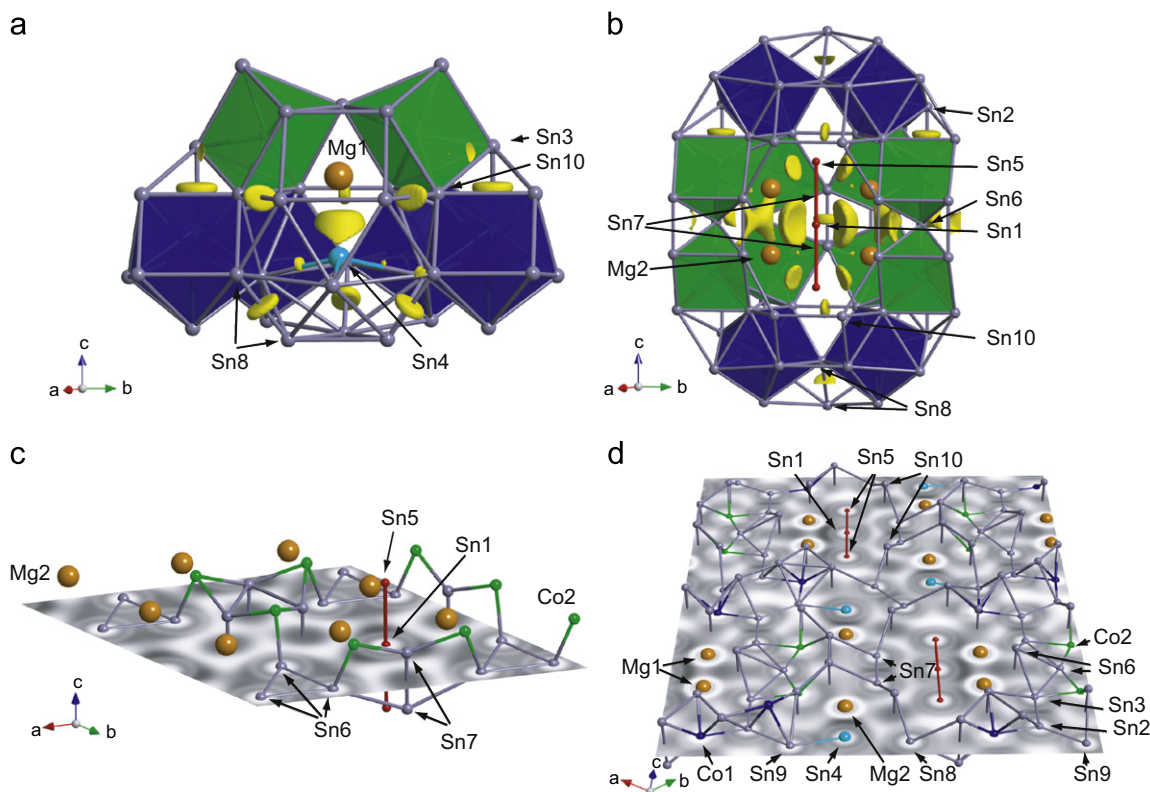
Fig. 6. ELF of $Mg_2Co_3Sn_{10+x}$ in the vicinity of the Mg atoms: (a) Mg1, $\eta = 0.5$; (b) Mg2, $\eta = 0.5$; (c) (001) layer at $z = 0.25$ through Sn1 with $-0.2 \leqslant x \leqslant 1.3$, $-0.3 \leqslant y \leqslant 1.2$; (d) (110) layer through Sn1 with $-0.2 \leqslant x \leqslant 1.3$, $-0.3 \leqslant y \leqslant 1.2$, and $0 \leqslant z \leqslant 1$. The values of ELF are shown as grey scales: the darker, the higher value of ELF. Please note that the atoms and ELF maxima in the front side of the structures in figures (a) and (b) are removed for sake of clarity.

Table 6
Atomic charges calculated for $Mg_2Co_3Sn_{10+x}$ according to Bader's analysis

Atom	Charge	Atom	Charge
Mg1	1.507(1)	Sn4	−0.399(6)
Mg2	1.474(1)	Sn5	−0.659(2)
Co1	−0.75(10)	Sn6	−0.431(11)
Co2	−1.148(7)	Sn7	−0.044(40)
Sn1	−1.220(1)	Sn8	0.285(19)
Sn2	0.240(3)	Sn9	0.278(10)
Sn3	0.069(1)	Sn10	0.080(11)

The observed features in $Mg_2Co_3Sn_{10+x}$ can be understood by an electron transfer from the Mg atoms mainly to the Sn1, Sn4, Sn5, and Sn6 atoms, introducing ionic and covalent bonding into the structure. The remaining Co and Sn atoms form a 3D framework, which is mainly of metallic character, as could also be derived from the DOS. Comparing bond length, compressibility and covalent bonding reveals that in $Mg_2Co_3Sn_{10+x}$ there is no direct correlation between these properties. According to the bonding analysis, the following bonds show a distinct covalent character (with corresponding distances and compressibility ratio, cf. (Table 5): Sn2–Sn3 (2.884(2) Å, 0.949(7)), Sn7–Sn7 (2.911(1) Å, 0.965(5)), Sn8–Sn8 (3.195(1) Å, 0.967(1)), and Sn10–Sn10 (3.381(1) Å, 0.954(1)). Surprisingly, also bonds well above a length of 3 Å are found to be covalent bonds (Sn8–Sn8, Sn10–Sn10). The bond length varies about 0.5 Å and none of the bond length compressibilities of the covalent bonds are above the $\pm 3\sigma$ level (Fig. 3). The anisotropic compressibility results there-

fore from the topology of the 3D metallic Co–Sn framework. Despite the presence of localized an delocalized chemical bonding, the properties of $Mg_2Co_3Sn_{10+x}$ are dominated by the metallic framework.

4. Conclusion

$Mg_2Co_3Sn_{10+x}$ can well be labelled complex metallic alloy. The presence of localized and delocalized chemical bonding reflects the complexity of its crystal structure. Built of a metallic 3D framework, it contains also covalently bonded Sn atoms and Mg ions. Nevertheless, the properties of this compound, like compressibility and magnetism are dominated by the framework.

References

[1] G. Krauss, R. Miletich, W. Steurer, Phil. Mag. Lett. 83 (2003) 525.
[2] T. Yamanaka, T. Fukuda, T. Hattori, H. Sumiya, Rev. Sci. Instrum. 72 (2001) 1458.
[3] G. Krauss, W. Steurer, J. Phys. Condens. Matter 16 (2004) 7769.
[4] W. Schreyer, G. Krauss, T.F. Fässler, Z. Anorg. Allg. Chem. 630 (2004) 2520.
[5] G. Krauss, H. Reifler, W. Steurer, Rev. Sci. Instrum. 76 (2005) 105104.
[6] Oxford Diffraction Ltd., CrysAlis Software System, Version 1.171.32.4, 2006.
[7] R.J. Angel, J. Appl. Cryst. 37 (2004) 486.
[8] R.J. Angel, Average V2.2, Virginia Tech, Blacksburgh, USA, 2003.
[9] R.J. Angel, Rev. Mineral. Geochem. 41 (2000) 35.
[10] G. Kresse, J. Furthmuller, J. Comput. Mater. Sci. 6 (1996) 15.

[11] G. Kresse, J. Furthmuller, Phys. Rev. B 54 (1996) 11169.
[12] P.E. Blochl, Phys. Rev. B 50 (1994) 17953.
[13] D. Vanderbilt, Phys. Rev. B 41 (1990) 7892.
[14] A. Savin, H.J. Flad, J. Flad, H. Preuss, H.G. von Schnering, Angew. Chem. Int. Ed. Engl. 31 (1992) 185.
[15] G. Henkelman, A. Arnaldsson, H. Johnsson, Comput. Mater. Sci. 36 (2006) 254.
[16] K. Momma, F. Izumi, Comm. Crystallogr. Comput. IUCr Newslett. 7 (2006) 106.
[17] A.-K. Larsson, M. Haeberlein, S. Lidin, U. Schwarz, J. Alloy Compd. 240 (1996) 79.
[18] A.-M. James, M.P. Lord, MacMillan's Chemical and Physical Data, MacMillan, London, 1992.
[19] V. Hlukhyy, S. Eck, T.F. Fässler, Inorg. Chem. 45 (2006) 7408.